Contraction-induced skeletal muscle FAT/CD36 trafficking and FA uptake is AMPK independent

J. Jeppesen,* P. H. Albers,* A. J. Rose,*,† J. B. Birk,* P. Schjerling,§ N. Dzamko, G. R. Steinberg,**,†† and B. Kiens[1],***

Copenhagen Muscle Research Center,* Molecular Physiology Group, Section of Human Physiology, Department of Exercise and Sport Science, and Institute of Sports Medicine,§ Bispebjerg Hospital, and Center for Healthy Aging, Faculty of Health Sciences, University of Copenhagen, Copenhagen, Denmark; Molecular Metabolic Control,† German Cancer Research Center, Heidelberg, Germany; St. Vincent's Institute of Medical Research and Department of Medicine,** University of Melbourne, Melbourne, Australia; and Department of Medicine,†† McMaster University, Hamilton, ON, Canada

Abstract The aim of this study was to investigate the molecular mechanisms regulating FA translocase CD36 (FAT/CD36) translocation and FA uptake in skeletal muscle during contractions. In one model, wild-type (WT) and AMP-dependent protein kinase kinase dead (AMPK KD) mice were exercised or extensor digitorum longus (EDL) and soleus (SOL) muscles were contracted, ex vivo. In separate studies, FAT/CD36 translocation and FA uptake in response to muscle contractions were investigated in the perfused rat hindlimb. Exercise induced a similar increase in skeletal muscle cell surface membrane FAT/CD36 content in WT (+34%) and AMPK KD (+37%) mice. In contrast, 5-aminoimidazole-4-carboxamide ribonucleoside only induced an increase in cell surface FAT/CD36 content in WT (+29%) mice. Furthermore, in the perfused rat hindlimb, muscle contraction induced a rapid (1 min, +15%) and sustained (10 min, +24%) FAT/CD36 relocation to cell surface membranes. The increase in cell surface FAT/CD36 protein content with muscle contractions was associated with increased FA uptake, both in EDL and SOL muscle from WT and AMPK KD mice and in the perfused rat hindlimb. This suggests that AMPK is not essential in regulation of FAT/CD36 translocation and FA uptake in skeletal muscle during contractions. However, AMPK could be important in regulation of FAT/CD36 distribution in other physiological situations.—Jeppesen, J., P. H. Albers, A. J. Rose, J. B. Birk, P. Schjerling, N. Dzamko, G. R. Steinberg, and B. Kiens. Contraction-induced skeletal muscle FAT/CD36 trafficking and FA uptake is AMPK independent. ***J. Lipid Res.*** **2011.** 52: **699–711.**

Supplementary key words fatty acid metabolism • fatty acid translocase CD36 • trafficking • AMP-dependent protein kinase

During submaximal exercise, plasma FAs are an important source of energy, accounting for ~60% of total substrate utilization in human subjects (1–3). Increases in FA utilization during exercise are facilitated by a rapid and sustained upregulation of skeletal muscle FA uptake by 5–15-fold (1, 4). This increase in skeletal muscle FA uptake during exercise results from a coordinated increase in rates of FA delivery, surface membrane FA transport, and intracellular substrate flux through mitochondrial β-oxidation or storage as intracellular lipids [for review, see (5)]. Skeletal muscle expresses multiple lipid binding proteins [for review, see (6)], such as the membrane-bound FA binding protein (7), the FA transport proteins (FATP1 and FATP4) (8, 9), and the FA translocase CD36 (FAT/CD36) (10), all of which have been implicated in the transsarcolemmal transport of FA uptake (9, 11, 12). The functional role of FAT/CD36 in long-chain FA plasma membrane transport is supported by studies reporting blunted uptake of the palmitic acid analog β-methyl-*p*-iodophenylpendadecanoic acid (^{123}I BMIPP) in cardiac muscle from humans with partial or total deficiency in FAT/CD36 protein (13–15). Furthermore, FA uptake in cardiac and skeletal muscle as well as adipocytes is reduced

Financial support from the Integrated Project Grant LSHM-CT-2004-005272 funded by the European Commission, the Danish Agency of Science Technology, and Innovation, the Ministry of Food, Agriculture, and Fisheries, and The Novo Nordisk Foundation (B.K.) is acknowledged. Funding from The National Health and Medical Research Council of Australia and the National Engineering and Research Council of Canada (G.R.S.) is acknowledged. Additional support was provided by a graduate scholarship from the National Heart Foundation (N.D.) and the Academy of Muscle Biology, Exercise, and Health and the Danish Agency for Science Technology and Innovation (J.J.). G.R.S. is a Canadian Research Chair in Metabolism, Obesity, and Type 2 Diabetes.

Manuscript received 30 March 2010 and in revised form 30 November 2010.

Published, JLR Papers in Press, February 6, 2011
DOI 10.1194/jlr.M007138

Abbreviations: ACC, acetyl carboxylase-CoA; AICAR, 5-aminoimidazole-4-carboxamide ribonucleoside; AMPK, AMP-dependent protein kinase; BCA, bicinchoninic acid; CaMK, calmodulin-dependent protein kinase; DG, diacylglycerol; EDL, extensor digitorum longus; ERK, extracellular signal-regulated kinase; FAT/CD36, FA translocase CD36; FATP1, FA transport protein 1; KO, knockout; SOL, soleus; TG, triacylglycerol; WT, wild-type.

[1]To whom correspondence should be addressed.
e-mail bkiens@ifi.ku.dk

Copyright © 2011 by the American Society for Biochemistry and Molecular Biology, Inc.

This article is available online at http://www.jlr.org

Downloaded from www.jlr.org by guest, on June 20, 2012

in CD36 knockout (KO) mice compared with their wild-type (WT) littermates (11, 16).

FAT/CD36 and potentially other lipid binding proteins function as dynamic regulators of FA transport by relocating from intracellular compartments to the plasma membrane in skeletal muscle in response to both muscle contractions (17, 18) and pharmacological activation of the AMP-dependent protein kinase (AMPK) by 5-aminoimidazole-4-carboxamide ribonucleoside (AICAR) (17). Furthermore, when CD36 KO mice were subjected to hindquarter perfusion, it was shown that the AICAR-induced increase in FA uptake was blunted in CD36 KO mice compared with their WT controls (11). In addition, FA uptake into skeletal muscle was increased 2.4-fold during AICAR infusion of rats (19). Taken together, these data suggest a functional role of AMPK in the dynamic regulation of FAT/CD36 trafficking and, ultimately, FA uptake. However, Turcotte, Raney, and Todd have shown that contraction-induced FAT/CD36 translocation and increases in FA uptake are prevented when the rat hindquarter is perfused with an inhibitor of the extracellular signal-regulated kinase (ERK) 1/2 and can occur independently of AMPK activation (20). The equivocal findings suggest the need for further evidence in order to elucidate the regulatory mechanism behind FAT/CD36 trafficking and the effect on FA uptake in skeletal muscle. Therefore, the aim of this study was to investigate the molecular mechanisms regulating FAT/CD36 translocation in skeletal muscle during contractions.

MATERIALS AND METHODS

All materials were from Sigma-Aldrich unless otherwise stated.

Experimental design and animals

To investigate the role of AMPK in the regulation of FAT/CD36 translocation, we used C57BL/6 mice overexpressing a kinase-dead Lys^{45}-Arg mutant AMPK α-2-protein, driven by the heart- and skeletal muscle-specific creatine kinase promoter, as described previously (21). The mice were a gift from Morris J. Birnbaum, Pennsylvania School of Medicine. Male hemizygous transgenic mice (AMPK KD) and WT mice (16–18 weeks of age) were used, and they were littermates from intercross breeding of hemizygous transgenic mice and WT mice.

In addition, to further delineate the signaling pathways involved, we investigated the time-dependent manner of FAT/CD36 translocation in relation to FA uptake and oxidation in skeletal muscle, using the perfused rat hindlimb model on male Wistar rats (200–250 g). All animals were maintained on a 10:14 h light-dark cycle and received standard rodent diet (Altromin no. 1324; Chr. Pedersen, Ringsted, Denmark) and water ad libitum. All experiments were approved by the Danish Animal Experimental Inspectorate and complied with the European Convention for the Protection of Vertebrate Animals Used for Experiments and Other Scientific Purposes.

Subcellular fractionation

Subcellular fractionation of rat and mouse skeletal muscle was performed as previously described in rats (22, 23). The mouse hindlimb muscles were removed and dissected free of connective tissue, nervous tissue, and visible fat. The muscles were minced and homogenized on ice three times (5 s each) using a Polytron homogenizer (PT3100; Kinematic, Switzerland) set at maximum speed (13,000 rpm) in 10 ml buffer containing 20 mM HEPES, 250 mM sucrose, 2 mM EDTA, 10 mM sodium fluoride, 20 mM sodium pyrophosphate, 3 mM benzamidine, 10 μg/ml aprotinin A, 10 μg/ml leupeptin, and 2 mM PMSF, pH 7.4. A small aliquot, 500 μl, of the homogenate was frozen and stored at −80°C for later production of lysate. The remaining homogenate was centrifuged at 2,000 *g* for 10 min (Hettich Zentrifugen, Germany). The supernatant was transferred to new tubes, and the pellet was resuspended in 5 ml of homogenization buffer, rehomogenized, and centrifuged again at 2,000 *g* for 10 min. The pellet, which contained mainly unhomogenized pieces of tissue, was discarded, and the two supernatants were pooled, filtered through double-layered gauze, and centrifuged at 12,000 *g*, in a Sorvall SS34 rotor (Thermo Fisher Scientific, Inc.) for 20 min. The 12,000 *g* pellet (P1) was resuspended in PBS with the cocktail of protease and phosphatase inhibitors listed above and saved for later analysis by Western blotting. The supernatant was centrifuged at 180,000 *g* for 90 min. The 180,000 *g* supernatant (cytosol fraction) was stored, and the pellet was resuspended in PBS with protease and phosphatase inhibitors, mechanically homogenized using a Teflon pestle, loaded on a 10–30% (wt/wt) continuous sucrose gradient, and centrifuged at 50,000 rpm for 55 min in an AH-650 Sorvall swing-out rotor (Thermo Fisher Scientific, Inc.). Gradients were harvested using a syringe and separated into eight fractions (F1–F8), starting from the bottom of the tube. The pellet of the sucrose gradient centrifugation (P2) was resuspended in PBS with protease and phosphatase inhibitors and analyzed together with the gradient fractions. All centrifugations were performed at 4°C.

Whole-cell lysate preparation

A 500 μl aliquot of homogenate saved prior to centrifugation and subcellular fractionation was supplemented with NP40 and NaCl to final concentrations of 1% NP40 and 150 mM NaCl, respectively. The homogenates were rehomogenized using a polytron at maximum speed (PT1200; Kinematic, Switzerland), mixed thoroughly by end-over-end rotation at 4°C for 60 min, and finally centrifuged at 16,000 *g* for 20 min at 4°C. The clarified supernatant (i.e., lysate) was removed and stored at −80°C until required. A small aliquot of each lysate was taken and diluted for determination of protein concentration prior to storage.

Exercise protocol

All mice were acclimatized three times on separate days to treadmill running, starting at day −5 prior to the experiment. Initially, mice were allowed to rest in the treadmill for 10 min and were then exercised by running 5 min at 10 m/min and 5 min at 17 m/min at 0% incline. On the experimental day, fed mice were randomized into either a nonexercised basal group or an exercised group. After 30 min at 17 m/min, mice were euthanized by cervical dislocation and the hindlimb muscles were quickly removed and used for subcellular fractionation, as described above.

AICAR stimulation

Fed mice were given an intraperitoneal injection with a bolus of saline (600 μl/100 g body weight) with or without AICAR (25 mg/100 g body weight). Blood samples were collected from the tail at time points 0, 30 min, and 60 min. After 60 min, mice were euthanized by cervical dislocation, and the hindlimb muscles were quickly removed and used for subcellular fractionation as described above.

FA uptake in isolated muscle ex vivo

All mice were anesthetized with sodium pentobarbital (5 mg/100 g body weight), and the extensor digitorum longus

Downloaded from www.jlr.org by guest, on June 20, 2012

(EDL) and soleus (SOL) muscles were carefully dissected tendon to tendon for muscle incubations, as previously described (24, 25).

FA metabolism experiments were conducted using procedures described previously (24, 25). Isolated EDL and SOL muscles were placed in warmed (30°C) Krebs-Henseleit buffer, pH 7.4, containing 2 mM pyruvate, 4% FA-free BSA (Bovogen; VIC, Australia), and 1 mM palmitic acid (Sigma; St. Louis, MO). Palmitic acid was dissolved in ethanol, and a small volume was added to the buffer (<1% total buffer volume) to achieve the desired palmitate concentration. For resting experiments with or without AICAR, the EDL and SOL muscle incubation volume was 2 ml, whereas for contraction experiments, the proximal and distal tendons of isolated EDL and SOL muscles were tied with silk suture and mounted to a force transducer in a 15 ml incubation reservoir (Radnoti; Monrovia, CA). After an initial incubation of 20 min, the incubation buffer was replaced with the same buffer described above supplemented with 0.5 μCi/ml of [1-^{14}C]palmitate (Amersham BioSciences; Little Chalfont, UK). For resting experiments, FA metabolism was determined over 90 min in the presence or absence of 2 mM AICAR. In contraction experiments, FA metabolism was measured in fused tetani of EDL (50 Hz, 350 ms pulse duration, 6 tetani/min) and SOL (30 Hz, 600 ms pulse duration, 18 tetani/min) over 25 min. This contraction protocol was selected because it has previously been demonstrated to maximally stimulate FA metabolism in isolated muscles (26). At the completion of the contraction protocol, muscles were removed, snap-frozen in liquid nitrogen, and stored at −80°C.

FA uptake was determined as the sum of [1-^{14}C]palmiate oxidation to $^{14}CO_2$ [reported elsewhere (27)] and incorporation of [1-^{14}C]palmitic acid into triacylglycerol (TG) and diacylglycerol (DG) in the muscles, as described previously (24). For FA oxidation experiments, gaseous $^{14}CO_2$ was liberated from the incubation media with 1 M acetic acid and trapped with vials containing 0.5 ml benzethonium hydroxide (Sigma; St. Louis, MO). Radioactivity in trapped $^{14}CO_2$ was determined by liquid scintillation counting using Ultima Gold (Perkin Elmer, MA). Frozen muscle strips were quickly weighed and homogenized in 2:1 chloroform-methanol, and 750 μl of the aqueous phase was subjected to liquid scintillation counting. Counts obtained within the aqueous phase were combined with the counts from trapped $^{14}CO_2$ to calculate rates of FA oxidation. The chloroform fraction of the muscle lysates containing the total lipids was gently evaporated under liquid N_2 and was redissolved in 50 μl of 2:1 chloroform-methanol containing 0.5 mg/ml of lipids (TG and DG; Sigma Chemical, St. Louis, MO) to identify the lipid bands on the silica gel plates. Twenty-five microliters of each sample was then spotted on an oven-dried silica gel plate (Fisher Scientific Canada; ON, Canada). Silica gel plates were placed in a sealed tank containing solvent (60:40:3 heptane-isopropyl ether-acetic acid) for 40 min. Plates were then permitted to dry, sprayed with dichlorofluorescein dye (0.02% w/v in ethanol), and visualized under long-wave ultraviolet light. The individual lipid bands were marked on the plate with a scalpel and scraped into vials for liquid scintillation counting.

Perfused rat hindlimb

On the day of the experiment, rats were anesthetized by an intraperitoneal injection of pentobarbital sodium (4–5 mg/100 g body weight). Surgery for two-legged perfusion was performed essentially as outlined by Ruderman, Houghton, and Hems (28). All perfusions were carried out with cell-free medium consisting of Krebs-Ringer bicarbonate buffer solution, 4% BSA (fraction V; Sigma-Aldrich, Copenhagen, Denmark) dialyzed twice for 24 h against 25 vol of Krebs-Ringer bicarbonate buffer solution (pore size 10–15 kDa), 550 μM palmitate, 542 nM [1-^{14}C]palmitic acid (PerkinElmer), and 6 mM glucose. The perfusion apparatus included an artificial lung by means of which the arterial perfusate was continuously gassed with a mixture of 95% O_2/5% CO_2. The O_2 pressure of the arterial perfusate was on average 545 ± 10 mmHg, pH 7.4 ± 0.1 (n = 16), and the perfusion pressure was 54 ± 1 mmHg (n = 16). The arterial perfusate was heated to a temperature of 35°C, resulting in a muscle temperature (calf muscle) of ~32°C. With respect to the viability of the presently used muscle preparation, it has previously been shown that muscle ATP and CrP values during 45 min of basal perfusion with a cell-free medium are not different from the values obtained from rested anesthetized rats (29). The first 50 ml of perfusate that passed through the hindlimbs was discarded, whereupon the hindlimbs were equilibrated for 20 min at a perfusion flow of 20 ml/min. The right leg of the rat was immobilized at the tibiopatellar ligament, and a hook electrode was placed around the sciatic nerve and connected to a D345 Powerstimulator (Digitimer Ltd.). The resting length of the gastrocnemius-soleus-plantaris muscle group was adjusted to obtain maximum active tension upon stimulation. Isometric muscle contractions were induced by stimulating the sciatic nerve electrically, as previously described (30, 31), with supramaximal trains 5–15 V adjusted to obtain full fiber recruitment, 50 Hz with impulse duration of 1 ms, delivered every 3 s. Muscles were stimulated to contract for 1 or 10 min. FA uptake and FA oxidation, ^{14}C and $^{14}CO_2$ radioactivities, respectively, were determined in duplicate, as previously described in detail (32, 33). P_{CO2}, P_{O2}, and pH were measured with an ABL-5 analyzer (Radiometer America; Westlake, OH). Arterial concentration of FA (544 ± 10 μmol/l, n = 16) and FA delivery (210 ± 5 nmol/min/g perfused muscle tissue, n = 16) were unchanged throughout the experiment. At the termination of the exercise, the resting and the stimulated gastrocnemius-plantaris muscles were removed and used for subcellular fractionation, as described above.

Muscle metabolites

Muscle glycogen content in rat and mouse skeletal muscle was determined as glycosyl units after acid hydrolysis (34).

Plasma metabolites

Glucose concentration in mouse plasma (from a pericardial blood sample) and in rat perfusate samples was measured enzymatically by use of the hexokinase and glucose-6-phosphate dehydrogenase reaction on a Roche/Hitachi 912 autoanalyzer (Roche Diagnostics A/S; Hvidovre, Denmark). FA concentration in mouse plasma and in the rat perfusate samples was measured using a colorimetric commercial assay kit (Wako Chemicals; Richmond, VA) using a COBAS FARA 2 autoanalyzer (Roche Diagnostics; Rotkreuz, Switzerland).

Analytical techniques

Protein concentration of the lysates, the P1, P2, and cytosol fractions was determined in triplicate using the bicinchoninic acid (BCA) method using BSA standards (Pierce) and BCA assay reagents (Pierce). A maximal coefficient of variance of 5% was accepted between replicates. All samples were heated (96°C) in laemmli buffer before being subjected to SDS-PAGE and immunoblotting. Total protein and phosphorylation levels of relevant proteins were determined by standard immunoblotting techniques. The primary antibodies used were anti-α_2-AMPK (kindly donated by D. G. Hardie, Dundee, UK), anti-transferrin receptor (Zymed Laboratories, Invitrogen), anti-GLUT1 (Affinity Bioreagents), anti-GLUT4 (Affinity Bioreagents), anti-DHPRα1 (Affinity Bioreagents), anti-FABPc (kindly donated by J. F. Glatz, Maastricht, The Netherlands), anti-triadin (Affinity Bioreagents),

Downloaded from www.jlr.org by guest, on June 20, 2012

anti-F_1ATPase-β (Santa-Cruz Biotech.), anti-FAT/CD36 (R and D Systems), anti-ERK1/2 (Cell Signaling Technology), and anti-CaMKII (BD Transduction Laboratory). The primary phospho-specific antibodies were anti-phospho-ERK TxY$^{202/204}$ (Cell Signaling Technology), anti-phospho-AMPK Thr^{172} (Cell Signaling Technology), anti-phospho-acetyl carboxylase-CoA (ACC) β (Upstate Biotechnology), anti-phospho-calcium/calmodulin-dependent protein kinase (CaMK) II Thr^{287} (Cell Signaling Technology). Secondary antibodies were from DakoCytomation (Denmark). Band intensity was quantified by Kodak imaging software (Kodak 1D 3.5). Preliminary experiments demonstrated that the amounts of protein loaded were within the dynamic range for the conditions used and the results obtained (data not shown).

α_1- and α_2-AMPK activity

α-Isoform-specific AMPK activity (pmol/min/mg protein) was measured in vitro in α_1-AMPK and α_2-AMPK immunoprecipitates (α_1- and α_2-AMPK antibodies were kindly donated by D. G. Hardie, University of Dundee, UK) from muscle lysate containing 200 μg protein using the AMARA peptide as substrate and a protocol identical to the one described previously (35).

Calculations and statistics

For mouse work, statistical evaluations were performed by two-way ANOVA with the Holm Sidak multiple comparison posthoc test used when the ANOVA revealed significant interactions between variables (intervention or genotype). For rat work, statistical evaluations were performed by either Student's *t*-test (effect of muscle contraction) or two-way ANOVA (effect of time) with the Holm Sidak multiple comparison posthoc test used when the ANOVA revealed significant interactions between variables. For statistical evaluation of fractionation work, the sum of arbitrary units from immunoblot scans of P1+P2 and F1–F8, respectively, were divided by the value for the lysate. Data are presented as means ± SEM. Statistical analyses and graph construction were performed using SigmaPlot v.11. Differences were considered to be significant when P was less than 0.05.

RESULTS

Characterization of subcellular fractionation on mouse skeletal muscle

The various fractions produced by the density-based separation of cellular membranes of mouse hindlimb muscle were characterized (**Fig. 1**). Markers of dense organelles such as mitochondria (β-subunit of the mitochondrial F_1-ATPase) and sarcoplasmic reticulum (triadin) were enriched in the heavy membrane fractions P1 and P2. Also, importantly, markers of surface membranes [GLUT1; dihydroxypyridine receptor α1 (t-tubuli)] were enriched in P1 and P2. Markers of recycling endosomes were enriched in the low-density membrane fractions F1–F8 (transferrin receptor, GLUT4), but these fractions were devoid of the markers of dense organelles. The soluble protein (cytosol) fraction was enriched with the cytosolic marker protein FABPc, and was devoid of markers of both dense- and light-membrane fractions, and the cytosolic marker was not detected in the membrane fractions. Altogether, this shows that this subcellular fractionation technique effectively allows distinction between surface and intracellular membrane compartments in mice, as we (22) and others (23) have previously shown in rats.

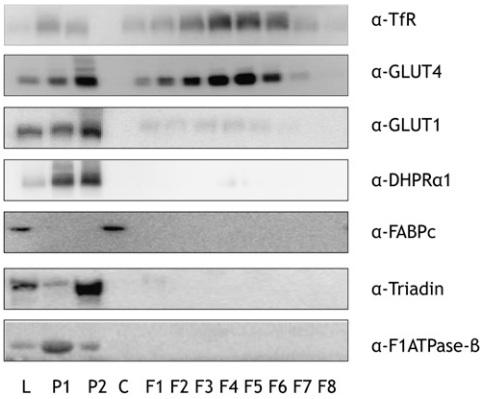

Fig. 1. Characterization of mouse skeletal muscle fractions. Mouse hindlimb muscles were excised and fractionated based upon a protocol of density-dependent separation. Protein concentrations of lysate (L), pellet 1 (P1), P2, and cytosol (C) were determined, equal protein amounts of these, as well as equal volume amounts of fractions 1–8 (F1–F8), were resolved by SDS-PAGE, and membranes were immunoblotted using antibodies specific for subcellular protein markers. These protein markers included transferrin receptor (TfR), glucose transporters 1 and 4 (GLUT1 and GLUT4, respectively), dihydroxypyridine receptor α-1 (DHPRα1), cytosolic fatty acid binding protein (FABPc), triadin/trisk95, and β-subunit of F_1-ATPase (F_1ATPase-β). Images of immunoblots are shown.

Effect of contractions and AICAR on skeletal muscle FAT/CD36 localization in WT and AMPK KD mice

Treadmill running for 30 min at 17 m/min induced redistribution of FAT/CD36 in mouse hindlimb muscle to fractions enriched in heavy membranes away from low-density membranes in both WT and AMPK KD mice (**Fig. 2**). In particular, a 34% ($P < 0.05$) and 37% ($P < 0.05$) increase in P1+P2 in WT and AMPK KD mice was obtained, and this was accompanied by a 32% ($P < 0.05$) and 39% ($P < 0.05$) decrease in low-density membranes F1–F8 in WT and AMPK KD mice, respectively (Fig. 2A, B). There was no significant difference in the redistribution pattern or in total FAT/CD36 protein expression between WT and AMPK KD mice (data not shown). AICAR, administrated intraperitoneally, induced a redistribution of FAT/CD36 in mouse hindlimb muscle to fractions enriched in heavy membranes away from low-density membranes in WT (**Fig. 3A**) but not in AMPK KD mice (Fig. 3B). In particular, there was a 25% increase in P1+P2 ($P < 0.05$) and a 30% decrease in F1–F8 ($P < 0.05$) in WT mice (Fig. 3A).

Skeletal muscle signaling in response to contraction and AICAR in WT and AMPK KD mice

In resting mouse hindlimb muscle, α_2-AMPK activity was reduced by 95% in AMPK KD mice compared with resting WT mice ($P < 0.001$), whereas, α_1-AMPK activity was similar between the genotypes. In WT mice, muscle α_2-AMPK activity was increased by exercise (87%, $P < 0.05$) and AICAR (38%, $P < 0.05$), but was unchanged in AMPK KD mice in response to either stimulus (**Fig. 4A, B**). There was no effect of exercise or AICAR on α_1-AMPK activity in either genotype (Fig. 4A, B). Basal phosphorylation of ACC-β Ser^{227} was reduced by ~50% ($P < 0.001$) in the AMPK KD mice compared with WT mice and increased with exercise

Downloaded from www.jlr.org by guest, on June 20, 2012

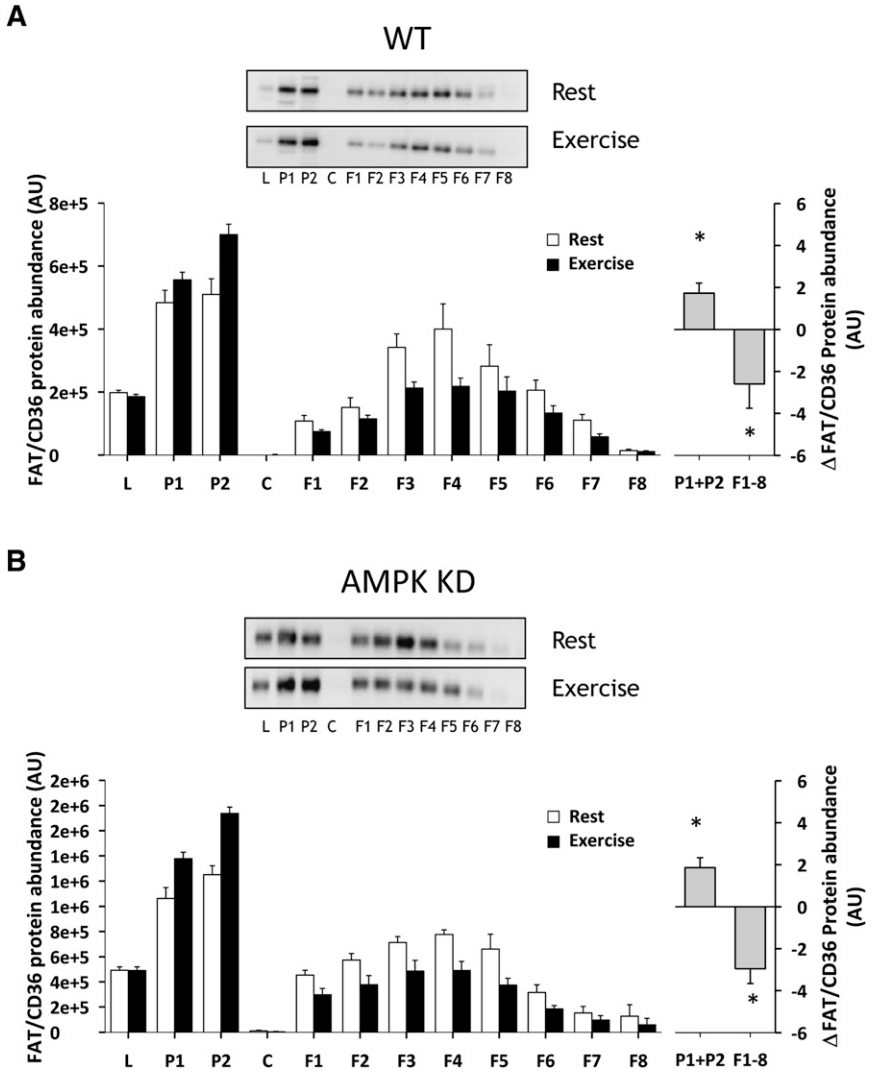

Fig. 2. Skeletal muscle FAT/CD36 translocates from intracellular membranes to surface membranes during treadmill running exercise. Fed WT and AMPK KD mice were randomized into either a nonexercised basal group or an exercised group (n = 7–8). After 30 min at 17 m/min of treadmill running, mice were euthanized by cervical dislocation, and the hindlimb muscles were quickly removed and used for subcellular fractionation. Exercise induced a similar FAT/CD36 translocation to cell surface membranes from intracellular compartments in WT (A) and AMPK KD (B) mice. There was no difference in the redistribution pattern between WT and AMPK KD mice. The left panels show the average data of each fraction and the right panels show the delta difference in abundance between conditions in surface membrane (P1+P2) and intracellular membranes (F1–F8). Data are means ± SEM, * significant difference from basal, $P < 0.05$. Representative images of immunoblots are shown. For statistical evaluation, see Materials and Methods section.

and AICAR in both WT ($P < 0.001$) and AMPK KD ($P < 0.05$) mice (Fig. 4C, D). Phosphorylation of ACC-β in resting and AICAR- or contraction-stimulated EDL and SOL muscle, ex vivo, is reported elsewhere (27). Muscle glycogen was lower in AMPK KD mice compared with WT controls, both at rest (58.9 ± 5.9 vs. 43.9 ± 5.0 mmol/kg/dry weight, $P < 0.001$) and after exercise (28.5 ± 6.2 vs. 12.4 ± 3.0 mmol/kg/dry weight, $P < 0.001$). Muscle glycogen was reduced with contraction in both WT and AMPK KD mice ($P < 0.01$).

Plasma metabolites

Plasma glucose (8.6 ± 0.3 vs. 9.3 ± 0.7 mM) and FA (1,112 ± 97 vs. 1,216 ± 74 μM) concentrations were similar in resting WT and AMPK KD mice. Exercise did not change plasma concentrations of glucose (8.8 ± 0.2 and 7.0 ± 1.8 mM) or FA (1,031 ± 75 and 1,278 ± 78 μM) in either WT or AMPK KD mice.

Effect of contraction and AICAR on ex vivo FA uptake in WT and AMPK KD mice

Resting FA uptake was similar in WT and AMPK KD mice in both SOL (5.2 ± 0.4 vs. 5.3 ± 0.4 pmol/min/mg muscle) (**Fig. 5A**) and EDL (2.3 ± 0.2 vs. 2.4 ± 0.4 pmol/min/mg muscle) (Fig. 5B) muscles. As expected, resting uptake of FAs was higher in SOL compared with EDL in both genotypes ($P < 0.001$) (Fig. 5A, B). In WT, but not in AMPK KD mice, AICAR increased FA uptake in SOL

Downloaded from www.jlr.org by guest, on June 20, 2012

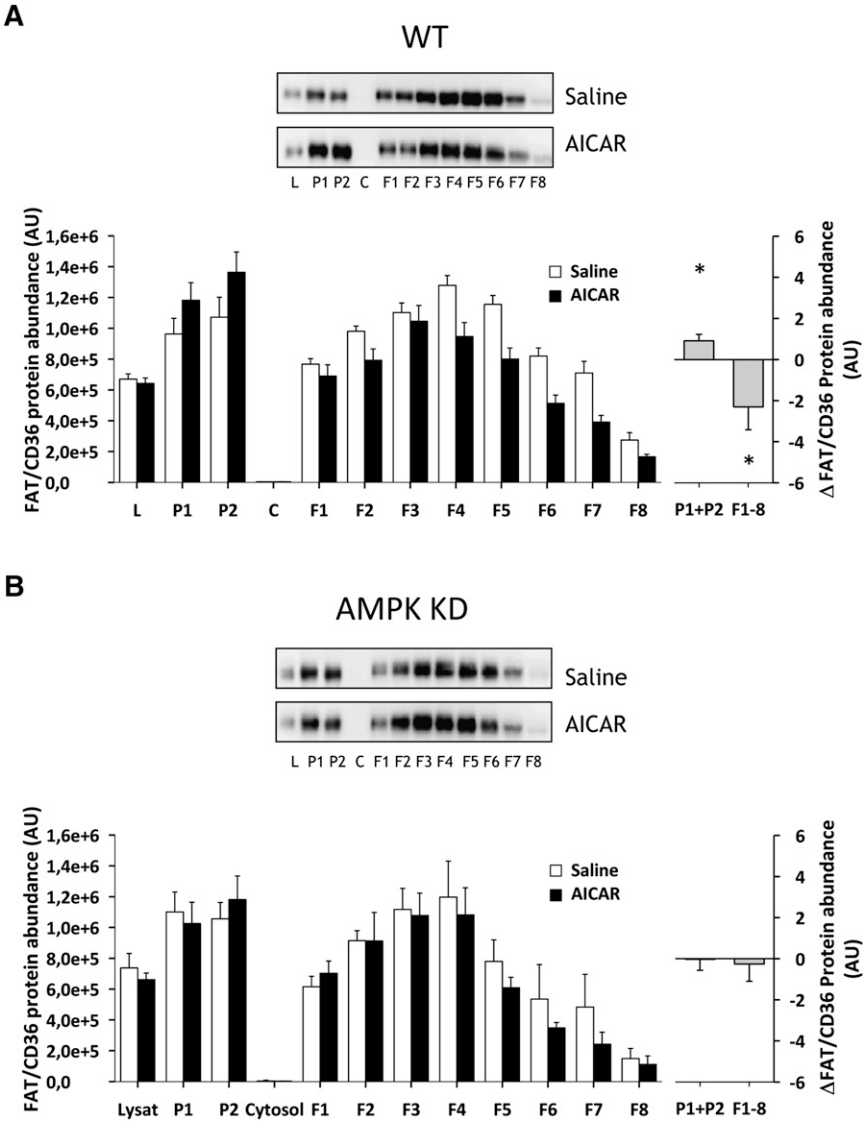

Fig. 3. AICAR induced skeletal muscle FAT/CD36 translocation from intracellular membranes to surface membranes in WT but not in AMPK KD mice. Fed WT and AMPK KD mice were given an intraperitoneal injection with a bolus of saline (600 μl/100 g body weight) with or without AICAR (25 mg/100 g body weight) (n = 8–9). After 60 min, mice were euthanized by cervical dislocation, and the hindlimb muscles were quickly removed and used for subcellular fractionation. AICAR induced a redistribution of FAT/CD36 to fractions enriched in heavy membranes away from low-density membranes in WT (A), but not in the AMPK KD mice (B). The left panels show the average data of each fraction and the right panels show the delta difference in abundance between conditions in surface membrane (P1+P2) and intracellular membranes (F1–F8). Data are means ± SEM, * significant difference from basal, $P < 0.05$. Representative images of immunoblots are shown. For statistical evaluation, see Materials and Methods section.

(22%, $P < 0.05$) and EDL (48%, $P < 0.05$) muscles (Fig. 5A, B). There was a tendency toward an AICAR effect in the EDL muscle from AMPK KD mice ($P = 0.07$) (Fig. 5B). Muscle contractions increased FA uptake in SOL and EDL muscle in both WT (144% and 485%, SOL and EDL, respectively, $P < 0.001$) and AMPK KD (218% and 473%, SOL and EDL, respectively, $P < 0.001$) mice, without any effect of genotype (Fig. 5A, B). The level of [1-^{14}C]palmitate incorporated into TG was higher in the resting SOL compared with EDL muscles in both WT and AMPK KD mice ($P < 0.05$), whereas incorporation into DG was similar between SOL and EDL muscle in both WT and AMPK KD mice (**Table 1**). There was no effect of genotype on resting TG or DG incorporation levels. Muscle contractions induced higher [1-^{14}C]palmitate incorporation into TG and DG in both SOL and EDL muscle in both WT and AMPK KD ($P < 0.001$) mice (Table 1), whereas AICAR did not significantly change the levels of [1-^{14}C]palmitate incorporated into TG and DG in WT or AMPK KD mice (data not shown).

Effect of contraction time on skeletal muscle FAT/CD36 localization in the perfused rat hindlimb

There was a redistribution of FAT/CD36 in rat posterior hindlimb muscle (gastrocnemius-plantaris) to fractions

Downloaded from www.jlr.org by guest, on June 20, 2012

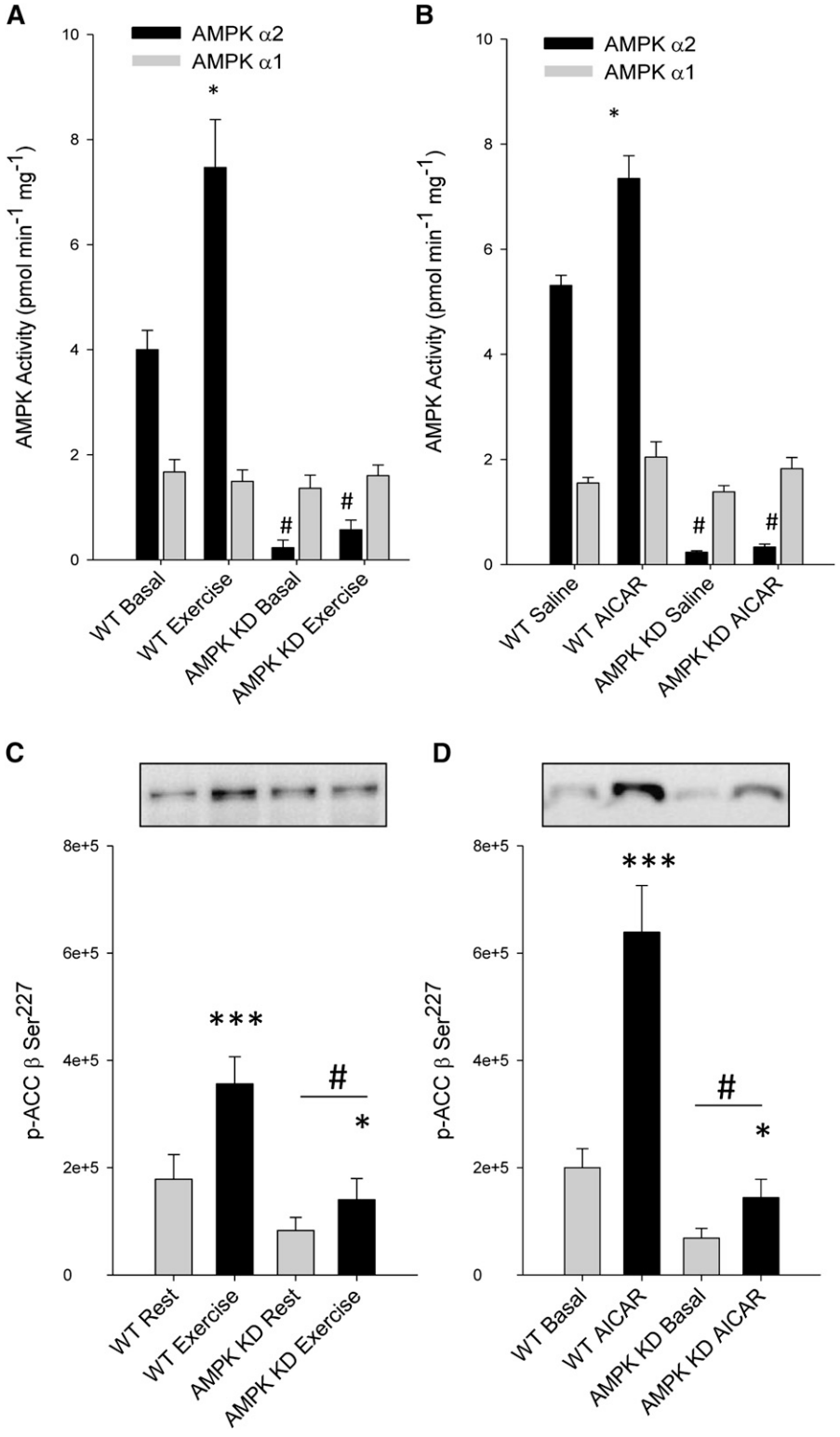

Fig. 4. Effect of AICAR and exercise on AMPK activity and ACC-β Ser^{227} phosphorylation in skeletal muscle. AMPKα_1 and -α_2 activities (A, B) and ACC-β Ser^{227} phosphorylation (C, D) were determined in gastrocnemius muscles from WT and AMPK KD mice under resting conditions or following treadmill exercise (n = 7–8, A and C) or after saline or AICAR injection (n = 8–9, B and D). Data are means ± SEM, */*** significant difference from basal, $P < 0.05/0.001$, # significant difference between genotypes, $P < 0.05$. For statistical evaluation, see Materials and Methods section.

Downloaded from www.jlr.org by guest, on June 20, 2012

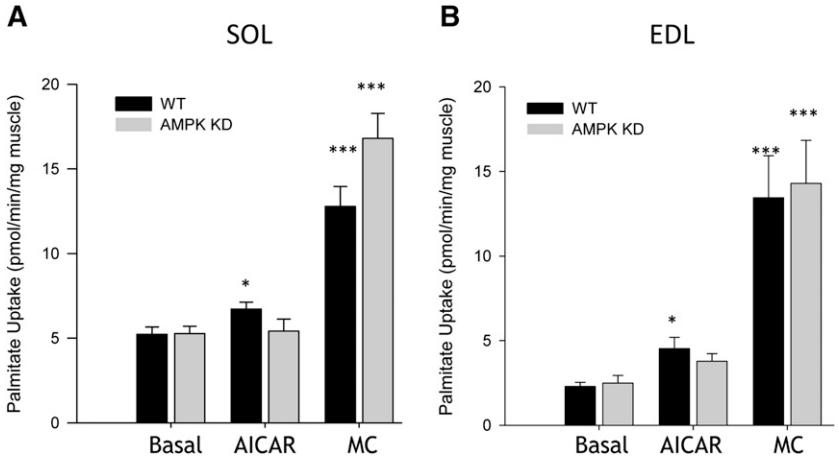

Fig. 5. FA uptake in isolated EDL and SOL muscle during ex vivo muscle contraction. WT and AMPK KD mice were anesthetized with sodium pentobarbital (5 mg/100 g body weight), and the EDL and SOL muscles were carefully dissected tendon to tendon for muscle incubations. SOL (A) (n = 9–12) and EDL (B) (n = 9–12) muscles were incubated at rest or subjected to either AICAR (2 mM) or contractions (MC), EDL (50 Hz, 350 ms pulse duration, 6 tetani/min) and SOL (30 Hz, 600 ms pulse duration, 18 tetani/min) over 25 min. Data are means ± SEM, */*** significant difference from basal, $P < 0.05/0.001$.

enriched in heavy membranes away from low-density membranes after 1 min (**Fig. 6A**) and 10 min (Fig. 6B) of electrically induced muscle contractions in situ. In particular, there was a 15% increase in heavy-density membrane FAT/CD36 protein content (P1+P2) after 1 min ($P < 0.05$) (Fig. 6A) and 24% after 10 min ($P < 0.05$) (Fig. 6B) of muscle contractions, compared with the resting contralateral control muscles. This was accompanied by a decrease in FAT/CD36 protein in the low-density membranes (F1–F8) of 19% after 1 min ($P < 0.05$) (Fig. 6A) and 25% after 10 min ($P < 0.05$) (Fig. 6B) of muscle contractions, respectively. There was no statistical difference between FAT/CD36 redistribution after 1 min and 10 min of muscle contraction.

Effect of contraction time on cellular signaling in the perfused rat hindlimb

One minute of in situ electrically stimulated muscle contractions (gastrocnemius-plantaris) increased CaMKII Thr^{287} phosphorylation (88%, $P < 0.001$, **Fig. 7A**) but did not affect phosphorylation of AMPK (Fig. 7B), ACC (Fig. 7C), or ERK (Fig. 7D), or the activity of AMPKα1 and -α2 (Fig. 7E, F). After 10 min of in situ muscle contractions, CaMKII Thr^{287} phosphorylation was still increased (44%, $P < 0.05$, Fig. 7A), along with phosphorylation of AMPK Thr^{172} (119%, $P < 0.01$, Fig. 7A), ACC-β Ser^{218} (83%, $P < 0.05$, Fig. 7B), and ERK1/2 TxY$^{202/204}$ (182%, $P < 0.01$). AMPKα_2 activity was increased by 80% ($P < 0.01$) after 10 min of muscle contractions, whereas AMPKα_1 activity was unchanged after both 1 and 10 min of muscle contractions. Skeletal muscle glycogen concentration was unchanged after 1 min (183 ± 10 vs. 166 ± 14 mmol/kg dry weight) of contraction, whereas it was lower (24%) after 10 min (160 ± 11 vs. 121 ± 14 mmol/kg dry weight, $P < 0.01$) of contractions compared with contralateral muscle glycogen levels.

TABLE 1. Incorporation of [1-^{14}C]palmitate into triacylglycerol and diacylglycerol in mouse soleus and extensor digitorum longus muscle, ex vivo

	SOL		EDL	
	Rest	MC	Rest	MC
	pmol/min/mg muscle			
WT				
TG	1.42 ± 0.17	5.78 ± 0.30[a]	0.42 ± 0.04[b]	2.00 ± 0.10[a]
DG	0.32 ± 0.03	1.58 ± 0.03[a]	0.34 ± 0.03	2.13 ± 0.12[a]
AMPK KD				
TG	1.22 ± 0.15	6.05 ± 0.50[a]	0.41 ± 0.07[b]	2.28 ± 0.33[a]
DG	0.34 ± 0.04	1.72 ± 0.13[a]	0.44 ± 0.06	2.43 ± 0.26[a]

SOL, soleus; EDL, extensor digitorum longus; WT, wild-type; DG, diacylglycerol; TG, triacylglycerol; AMPK, AMP-dependent protein kinase. There was no effect of genotype in resting (Rest) TG or DG incorporation levels. Muscle contractions (MC) induced higher [1-^{14}C] palmitate incorporation into TG and DG in both SOL and EDL muscle in both WT and AMPK KD mice. Data are means ± SEM. For statistical evaluation, see Materials and Methods section.

[a] Significant difference from basal, $P < 0.001$.

[b] Significant difference between muscle types, $P < 0.05$.

Effect of contraction time on FA uptake and oxidation in the perfused rat hindlimb

FA acid uptake in the perfused rat hindlimb muscle was increased 33% and 36% after 1 min (11.3 ± 0.6 vs. 15.1 ± 1.4 nmol/min/g, $P < 0.05$) and 10 min (11.1 ± 0.8 vs. 15.1 ± 1.4 nmol/min/g, $P < 0.05$) of muscle contractions, respectively (**Fig. 8A**). There was no difference in the contraction-induced increase in skeletal muscle FA uptake between 1 min and 10 min of contractions (Fig. 8A). FA oxidation was similar between rest and 1 min of muscle contractions (0.37 ± 0.03 vs. 0.46 ± 0.04 nmol/min/g), but increased 73% after 10 min (0.34 ± 0.03 vs. 0.59 ± 0.05 nmol/min/g, $P < 0.001$) of muscle contractions (Fig. 8B).

DISCUSSION

The purpose of the present study was to investigate FAT/CD36 trafficking in skeletal muscle and whether this process was AMPK dependent. Two animal models were used to investigate FAT/CD36 translocation and FA

Downloaded from www.jlr.org by guest, on June 20, 2012

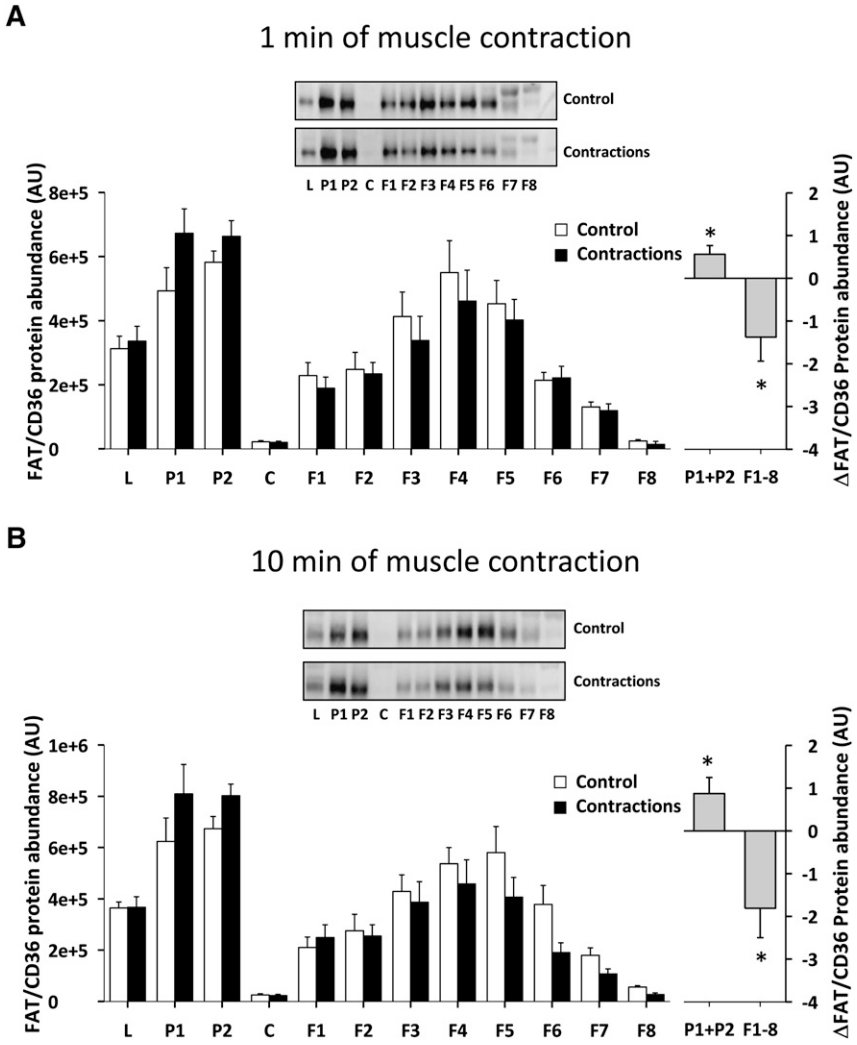

Fig. 6. Skeletal muscle FAT/CD36 translocates rapidly in the perfused rat hindlimb muscle during contractions. Rats were anesthetized by an intraperitoneal injection of pentobarbital sodium (4–5 mg/100 g body weight), and surgery for two-legged perfusion was performed. In one leg, isometric muscle contractions were induced in the gastrocnemius-plantaris muscle by stimulating the sciatic nerve electrically with supramaximal trains 5–15 V adjusted to obtain full fiber recruitment, 50 Hz with impulse duration of 1 ms, delivered every 3 s. Muscles were stimulated to contract for 1 or 10 min. There was a redistribution of FAT/CD36 to fractions enriched in heavy membranes away from low-density membranes after 1 min (A) (n = 6) and 10 min (B) (n = 6) of electrically induced muscle contraction compared with the resting contralateral control muscles. The left panels show the average data of each fraction and the right panels show the delta difference in abundance between conditions in surface membrane (P1+P2) and intracellular membranes (F1–F8). Data are means ± SEM, * significant difference from basal, $P < 0.05$. Representative images of immunoblots are shown. For statistical evaluation see Materials and Methods section.

uptake during muscle contractions/exercise. In one model, WT and AMPK KD mice performed treadmill exercise or were injected with AICAR; isolated SOL and EDL muscle were subjected to either contraction or AICAR stimulation, ex vivo. In the AMPK KD mice, activation of muscle AMPK during exercise was prevented by a skeletal- and heart muscle-specific expression of a kinase dead α_2-AMPK construct (21). In another model, we used the perfused rat hindlimb preparation (28) to investigate the time course of FAT/CD36 translocation and FA uptake in response to muscle contractions in situ. The major findings were that muscle contractions induced a rapid, AMPK-independent, FAT/CD36 relocation from intracellular compartments to cell surface membranes (Figs. 2, 6). This change in cell surface FAT/CD36 protein was associated with an increase in FA uptake (Figs. 5, 8). However, under nonexercising conditions, the effects of AICAR on FAT/CD36 translocation was eliminated in AMPK KD mice. These data suggest that AMPK could be an important regulator of FAT/CD36 translocation under some physiological conditions, but that during muscle contractions, factors independent of AMPK control this process.

The mechanisms initiating the relocation of FAT/CD36 from intracellular membranes to surface membranes are unclear. Several studies have suggested that AMPK is an important regulator of FAT/CD36 translocation in both

Downloaded from www.jlr.org by guest, on June 20, 2012

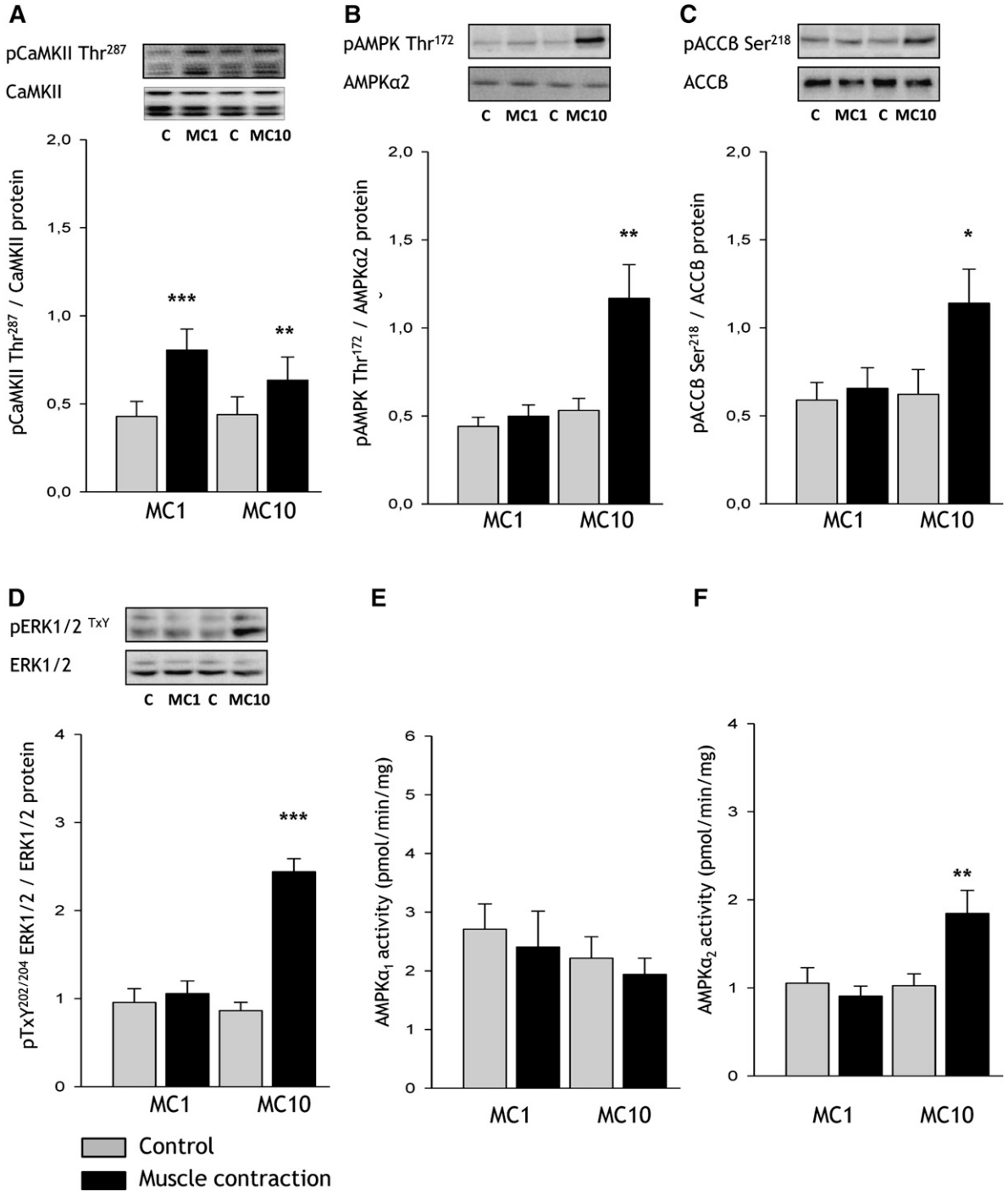

Fig. 7. Skeletal muscle signaling with contraction stimuli in the perfused rat hindlimb. Rats were anesthetized by an intraperitoneal injection of pentobarbital sodium (4–5 mg/100 g body weight), and surgery for two-legged perfusion was performed. Rats were subjected to sciatic nerve-induced contractions for either 1 (MC1) or 10 (MC10) min (n = 6) in situ, after which posterior hindlimb muscles (i.e., gastrocnemius and plantaris) from resting as well as stimulated conditions were excised. Phosphorylation of (A) calcium/calmodulin-dependent protein kinase II (CaMKIIThr^{287}), (B) AMP-dependent protein kinase (AMPK) Thr^{172}, (C) acetyl-CoA carboxylase (ACC) β Ser^{218}, (D) extracellular-regulated protein kinase (ERK) TxY$^{202/204}$, as well as AMPK α_1 (E) and α_2 activities (F) were determined in muscle lysates. Data are means ± SEM, */**/*** significant difference from basal, $P < 0.05/0.01/0.001$. Representative images of immunoblots are shown. MC, muscle contractions. For statistical evaluation, see Materials and Methods section.

skeletal muscle and heart muscle (17, 18, 36, 37). During muscle contractions, FAT/CD36 translocation to the plasma membrane has been shown in rat gastrocnemius muscle (17, 18), and the increase of FAT/CD36 in the plasma membrane has been associated with an increase in cellular FA transport (18, 38). Based on the findings from studies using muscle contractions and/or pharmacological approaches, it has been suggested that AMPK could be a major regulator of contraction-induced FAT/CD36 translocation in skeletal muscle (11, 17). In the present

Downloaded from www.jlr.org by guest, on June 20, 2012

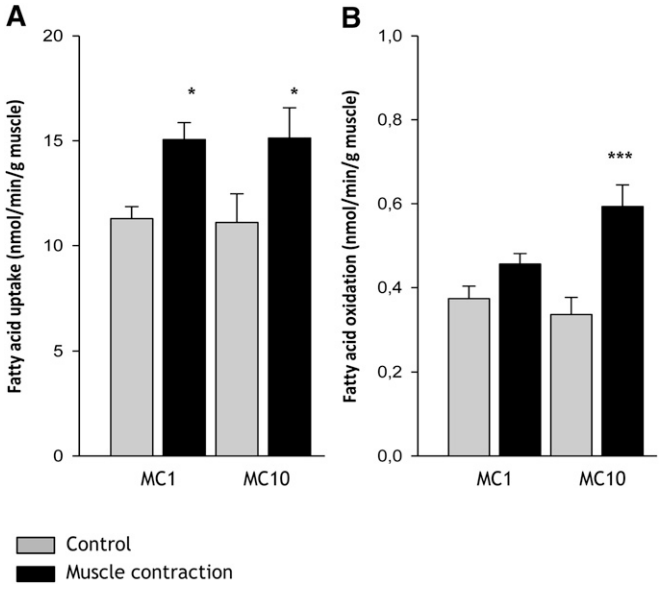

Fig. 8. FA uptake and oxidation during muscle contraction in the perfused rat hindlimb. Rats were anesthetized by an intraperitoneal injection of pentobarbital sodium (4–5 mg/100 g body weight), and surgery for two-legged perfusion was performed. Rats were subjected to sciatic nerve-induced contractions for either 1 min (MC 1) or 10 min (MC 10) (n = 8), in situ. FA uptake and oxidation were measured as arterial – venous differences in [^{14}C] and [$^{14}CO_2$], respectively. Skeletal muscle FA uptake was increased after 1 min and 10 min of muscle contractions, (A), whereas FA oxidation was similar between rest and 1 min of muscle contractions, but increased 73% after 10 min of muscle contractions (B). Data are means ± SEM, */*** significant difference from basal, $P < 0.05/0.001$. For statistical evaluation, see Materials and Methods section.

study, it was, however, demonstrated that α_2-AMPK is not essential in regulation of FAT/CD36 translocation, at least during muscle contractions, because FAT/CD36 protein content increased 30–40% in cell surface membranes (P1+P2) and correspondingly decreased 30–40% in the intracellular compartments (F1–F8) in both WT and AMPK KD mice after 30 min of treadmill running exercise at the same absolute running speed (Fig. 2). Interestingly, we recently observed similar findings in regard to GLUT4 translocation after treadmill running exercise (39). In the study by Maarbjerg et al., alternative exercise-sensitive signaling pathways, including CaMKII, Trisk95, p38 MAPK, and ERK1/2, were not increased in AMPK KD muscles during treadmill exercise at the same relative workloads (39). However, Dzamko et al., using in situ electrically stimulated contractions of mouse tibialis anterior muscle, found that several protein kinases in the p38 MAPK family, including ERK1/2, were upregulated in the AMPK KD mice, compared with their WT littermates (27). This discrepancy between the two studies is probably due to the much greater relative workload for the AMPK KD mice muscle during in situ muscle contractions compared with treadmill exercise. Therefore, because we examined FAT/CD36 translocation during treadmill exercise, it seems unlikely that upregulation of alternative signaling pathways could have contributed to the maintenance of FA uptake in the AMPK KD mice.

To further understand the dynamics of FAT/CD36 translocation during muscle contractions, we performed a muscle contraction time course experiment, using electrically stimulated muscle contractions in situ in the perfused rat hindlimb. Here we observed that FAT/CD36 translocation was a rapid (i.e., within 1 min) and sustained process during muscle contractions (Fig. 6). Furthermore, FAT/CD36 translocation occurred prior to the activation of AMPK and its downstream target, ACC-β (Figs. 6, 7). This observation supports the genetic evidence from the present study. Thus, taken together, these data suggest that α_2-AMPK is not an essential regulator of FAT/CD36 translocation to the surface membranes during muscle contractions.

The role of AMPK in the regulation of FA uptake in muscle has primarily been investigated using pharmacological approaches (11, 19, 40). Accordingly, it was shown that infusion of AICAR increased FA uptake into skeletal and heart muscle during a euglycemic clamp (19, 40). To determine the functional effect of blunted AMPK activity on FA uptake in skeletal muscle, we isolated SOL and EDL muscle from WT and AMPK KD mice and measured FA uptake ex vivo. FA uptake was similar in AMPK KD mice and their WT littermates in isolated SOL and EDL muscle, both at rest and during muscle contraction (Fig. 5). When muscles were incubated with AICAR, FA uptake increased only in WT muscles. This suggests that AMPK could be a regulator of FA uptake in resting (nonexercising) skeletal muscle. Due to the low amount of muscle tissue, we were unable to determine whether the AICAR- (only WT) or contraction- (WT and AMPK KD) induced increase in FA uptake was dependent on FAT/CD36 translocation. Interestingly, it was demonstrated in the perfused mouse hindlimb that AICAR-induced increase in FA uptake was blunted in CD36 KO mice compared with their WT littermates (11). Whether this is similar in isolated EDL and SOL muscle has yet to be determined. Because a direct comparison of in vivo exercise-induced FAT/CD36 translocation with ex vivo contraction-induced FA uptake is difficult, we applied the perfused rat hindlimb model to directly compare the two. One minute of muscle contractions induced a rapid FAT/CD36 translocation (i.e., within 1 min) (Fig. 6). Similarly, we observed that muscle contractions increased FA uptake in the perfused rat hindlimb, measured as arterial-venuos differences in [1-^{14}C]palmitate across the rat hindlimb (Fig. 8). Altogether, these data suggest that during muscle contraction, FA uptake and FAT/CD36 translocation in skeletal muscle are rapid processes occurring simultaneously and independent of AMPK. The delayed onset of increased FA oxidation, compared with the rapid increase in FA uptake observed in the present study (Fig. 8), supports the notion that plasma FA uptake in skeletal muscle is not limiting for FA oxidation during the onset of muscle contractions/exercise in healthy human subjects (41).

Based on the findings in the present study, it is suggested that cellular mechanisms other than AMPK are involved in the regulation of exercise/contraction-induced FAT/CD36 translocation and FA uptake in skeletal muscle. In

Downloaded from www.jlr.org by guest, on June 20, 2012

support of these findings, Raney and Turcotte (42) and Raney et al. (43) have shown that increased FA uptake and FA oxidation during low-intensity muscle contractions occur independently of AMPK activation. Furthermore, they suggested that ERK1/2 may be a primary regulator of FAT/CD36 translocation and FA uptake (20). However, in the present study, FAT/CD36 translocation occurred rapidly, before changes in ERK1/2 and AMPK activation, suggesting that neither ERK1/2 nor AMPK are essential for FAT/CD36 translocation or FA uptake during contraction in rat hindlimb muscle (Figs. 6, 7). Although the findings from the present study cannot exclude AMPK as a potential regulator of FAT/CD36 translocation under other physiological conditions, the rapidity of FAT/CD36 translocation and change in FA uptake observed, without changes in AMPK activation, suggests that AMPK is not the primary initiator of FA uptake in skeletal muscle. In regard to muscle contraction, calcium-sensitive signaling is an obviously attractive candidate for regulating metabolism and thus also FAT/CD36 translocation and FA uptake. Accordingly, it has been demonstrated that both CaMKII and protein kinase C were activated rapidly at the onset of muscle contractions (30, 44). In line with this, we (J. Jeppesen, P. H. Albers, and B. Kiens, unpublished observation) and others (36) recently observed that caffeine, a stimulator of sarcoplasmatic reticulum calcium release, induced translocation of FAT/CD36 from intracellular membranes to cell surface membranes in gastrocnemius muscle, and this was associated with an increase in FA uptake in the perfused rat hindlimb. In addition, Raney and Turcotte recently showed that the CaMKII inhibitor KN93 inhibited caffeine (3 mM)-induced increase in FA uptake in the perfused rat hindlimb (45). Thus, one could speculate that the rapid and sustained FAT/CD36 translocation and increase in FA uptake during muscle contraction could be mediated by calcium-induced signaling, possibly CaMKII, in rats. However, because 3 mM caffeine also has been shown to increase AMPK-dependent glucose uptake (46), a potential AMPK effect in these models cannot be ruled out. In addition, we (J. Jeppesen, P. H. Albers, and B. Kiens, unpublished observation) and others (30) have observed that other calcium-sensitive kinases, such as protein kinase C, are also activated rapidly during muscle contractions (30), and that therefore the role of calcium-sensitive signaling in regard to FAT/CD36 translocation and FA metabolism warrants further study.

In summary, treadmill running exercise induced a relocation of FAT/CD36 from intracellular compartments to cell surface membranes in skeletal muscle from both WT and AMPK KD mice. Furthermore, muscle contractions in situ induced a rapid and sustained FAT/CD36 relocation in the perfused rat hindlimb prior to activation of AMPK. In both models, the change in cell surface FAT/CD36 protein was associated with an increase in FA uptake. This suggests that AMPK is not essential in regulation of FAT/CD36 translocation and FA uptake in skeletal muscle during contractions. However, because AICAR induced a FAT/CD36 translocation in an AMPK-dependent manner, AMPK could potentially be important in the regulation of FAT/CD36 distribution under nonexercising conditions.

The authors are thankful to Dr. Erik A. Richter and Dr. Jørgen F. P. Wojtaszewski for qualified advice and help during the whole process of this project. The authors also acknowledge the skilled technical assistance of Irene B. Nielsen and Betina Bolmgren.

REFERENCES

1. Roepstorff, C., C. H. Steffensen, M. Madsen, B. Stallknecht, I. L. Kanstrup, E. A. Richter, and B. Kiens. 2002. Gender differences in substrate utilization during submaximal exercise in endurance-trained subjects. *Am. J. Physiol. Endocrinol. Metab.* **282:** E435–E447.
2. Stellingwerff, T., H. Boon, R. A. Jonkers, J. M. Senden, L. L. Spriet, R. Koopman, and L. J. van Loon. 2007. Significant intramyocellular lipid use during prolonged cycling in endurance-trained males as assessed by three different methodologies. *Am. J. Physiol. Endocrinol. Metab.* **292:** E1715–E1723.
3. Romijn, J. A., E. F. Coyle, L. S. Sidossis, A. Gastaldelli, J. F. Horowitz, E. Endert, and R. R. Wolfe. 1993. Regulation of endogenous fat and carbohydrate metabolism in relation to exercise intensity and duration. *Am. J. Physiol.* **265:** E380–E391.
4. Burguera, B., D. Proctor, N. Dietz, Z. Guo, M. Joyner, and M. D. Jensen. 2000. Leg free fatty acid kinetics during exercise in men and women. *Am. J. Physiol. Endocrinol. Metab.* **278:** E113–E117.
5. Kiens, B. 2006. Skeletal muscle lipid metabolism in exercise and insulin resistance. *Physiol. Rev.* **86:** 205–243.
6. Glatz, J. F., J. J. Luiken, and A. Bonen. 2010. Membrane fatty acid transporters as regulators of lipid metabolism: implications for metabolic disease. *Physiol. Rev.* **90:** 367–417.
7. Stremmel, W., G. Strohmeyer, F. Borchard, S. Kochwa, and P. D. Berk. 1985. Isolation and partial characterization of a fatty acid binding protein in rat liver plasma membranes. *Proc. Natl. Acad. Sci. USA.* **82:** 4–8.
8. Schaffer, J. E., and H. F. Lodish. 1994. Expression cloning and characterization of a novel adipocyte long chain fatty acid transport protein. *Cell.* **79:** 427–436.
9. Stahl, A., D. J. Hirsch, R. E. Gimeno, S. Punreddy, P. Ge, N. Watson, S. Patel, M. Kotler, A. Raimondi, L. A. Tartaglia, et al. 1999. Identification of the major intestinal fatty acid transport protein. *Mol. Cell.* **4:** 299–308.
10. Abumrad, N. A., M. R. el-Maghrabi, E. Z. Amri, E. Lopez, and P. A. Grimaldi. 1993. Cloning of a rat adipocyte membrane protein implicated in binding or transport of long-chain fatty acids that is induced during preadipocyte differentiation. Homology with human CD36. *J. Biol. Chem.* **268:** 17665–17668.
11. Bonen, A., X. X. Han, D. D. Habets, M. Febbraio, J. F. Glatz, and J. J. Luiken. 2007. A null mutation in skeletal muscle FAT/CD36 reveals its essential role in insulin- and AICAR-stimulated fatty acid metabolism. *Am. J. Physiol. Endocrinol. Metab.* **292:** E1740–E1749.
12. Clarke, D. C., D. Miskovic, X. X. Han, J. Calles-Escandon, J. F. Glatz, J. J. Luiken, J. J. Heikkila, and A. Bonen. 2004. Overexpression of membrane-associated fatty acid binding protein (FABPpm) in vivo increases fatty acid sarcolemmal transport and metabolism. *Physiol. Genomics.* **17:** 31–37.
13. Tanaka, T., T. Nakata, T. Oka, T. Ogawa, F. Okamoto, Y. Kusaka, K. Sohmiya, K. Shimamoto, and K. Itakura. 2001. Defect in human myocardial long-chain fatty acid uptake is caused by FAT/CD36 mutations. *J. Lipid Res.* **42:** 751–759.
14. Kintaka, T., T. Tanaka, M. Imai, I. Adachi, I. Narabayashi, and Y. Kitaura. 2002. CD36 genotype and long-chain fatty acid uptake in the heart. *Circ. J.* **66:** 819–825.
15. Nozaki, S., T. Tanaka, S. Yamashita, K. Sohmiya, T. Yoshizumi, F. Okamoto, Y. Kitaura, C. Kotake, H. Nishida, A. Nakata, et al. 1999. CD36 mediates long-chain fatty acid transport in human myocardium: complete myocardial accumulation defect of radiolabeled long-chain fatty acid analog in subjects with CD36 deficiency. *Mol. Cell. Biochem.* **192:** 129–135.
16. Coburn, C. T., F. F. Knapp, Jr., M. Febbraio, A. L. Beets, R. L. Silverstein, and N. A. Abumrad. 2000. Defective uptake and utilization of long chain fatty acids in muscle and adipose tissues of CD36 knockout mice. *J. Biol. Chem.* **275:** 32523–32529.

Downloaded from www.jlr.org by guest, on June 20, 2012

17. Jeppesen, J., P. Albers, J. J. Luiken, J. F. Glatz, and B. Kiens. 2009. Contractions but not AICAR increase FABPpm content in rat muscle sarcolemma. *Mol. Cell. Biochem.* **326:** 45–53.
18. Bonen, A., J. J. Luiken, Y. Arumugam, J. F. Glatz, and N. N. Tandon. 2000. Acute regulation of fatty acid uptake involves the cellular redistribution of fatty acid translocase. *J. Biol. Chem.* **275:** 14501–14508.
19. Shearer, J., P. T. Fueger, J. N. Rottman, D. P. Bracy, P. H. Martin, and D. H. Wasserman. 2004. AMPK stimulation increases LCFA but not glucose clearance in cardiac muscle in vivo. *Am. J. Physiol. Endocrinol. Metab.* **287:** E871–E877.
20. Turcotte, L. P., M. A. Raney, and M. K. Todd. 2005. ERK1/2 inhibition prevents contraction-induced increase in plasma membrane FAT/CD36 content and FA uptake in rodent muscle. *Acta Physiol. Scand.* **184:** 131–139.
21. Mu, J., J. T. Brozinick, Jr., O. Valladares, M. Bucan, and M. J. Birnbaum. 2001. A role for AMP-activated protein kinase in contraction- and hypoxia-regulated glucose transport in skeletal muscle. *Mol. Cell.* **7:** 1085–1094.
22. Rose, A. J., J. Jeppesen, B. Kiens, and E. A. Richter. 2009. Effects of contraction on localization of GLUT4 and v-SNARE isoforms in rat skeletal muscle. *Am. J. Physiol. Regul. Integr. Comp. Physiol.* **297:** R1228–R1237.
23. Zhou, M., L. Sevilla, G. Vallega, P. Chen, M. Palacin, A. Zorzano, P. F. Pilch, and K. V. Kandror. 1998. Insulin-dependent protein trafficking in skeletal muscle cells. *Am. J. Physiol.* **275:** E187–E196.
24. Steinberg, G. R., A. Bonen, and D. J. Dyck. 2002. Fatty acid oxidation and triacylglycerol hydrolysis are enhanced after chronic leptin treatment in rats. *Am. J. Physiol. Endocrinol. Metab.* **282:** E593–E600.
25. Steinberg, G. R., and D. J. Dyck. 2000. Development of leptin resistance in rat soleus muscle in response to high-fat diets. *Am. J. Physiol. Endocrinol. Metab.* **279:** E1374–E1382.
26. Dyck, D. J., and A. Bonen. 1998. Muscle contraction increases palmitate esterification and oxidation and triacylglycerol oxidation. *Am. J. Physiol.* **275:** E888–E896.
27. Dzamko, N., J. D. Schertzer, J. G. Ryall, R. Steel, S. L. Macaulay, S. Wee, Z. P. Chen, B. J. Michell, J. S. Oakhill, M. J. Watt, et al. 2008. AMPK-independent pathways regulate skeletal muscle fatty acid oxidation. *J. Physiol.* **586:** 5819–5831.
28. Ruderman, N. B., C. R. Houghton, and R. Hems. 1971. Evaluation of the isolated perfused rat hindquarter for the study of muscle metabolism. *Biochem. J.* **124:** 639–651.
29. Wojtaszewski, J. F., S. B. Jorgensen, Y. Hellsten, D. G. Hardie, and E. A. Richter. 2002. Glycogen-dependent effects of 5-aminoimidazole-4-carboxamide (AICA)-riboside on AMP-activated protein kinase and glycogen synthase activities in rat skeletal muscle. *Diabetes.* **51:** 284–292.
30. Richter, E. A., P. J. Cleland, S. Rattigan, and M. G. Clark. 1987. Contraction-associated translocation of protein kinase C in rat skeletal muscle. *FEBS Lett.* **217:** 232–236.
31. Richter, E. A., L. P. Garetto, M. N. Goodman, and N. B. Ruderman. 1984. Enhanced muscle glucose metabolism after exercise: modulation by local factors. *Am. J. Physiol.* **246:** E476–E482.
32. Turcotte, L. P., B. Kiens, and E. A. Richter. 1991. Saturation kinetics of palmitate uptake in perfused skeletal muscle. *FEBS Lett.* **279:** 327–329.
33. Turcotte, L. P., C. Petry, B. Kiens, and E. A. Richter. 1998. Contraction-induced increase in Vmax of palmitate uptake and oxidation in perfused skeletal muscle. *J. Appl. Physiol.* **84:** 1788–1794.
34. Passonneau, J. V., P. D. Gatfield, D. W. Schulz, and O. H. Lowry. 1967. An enzymic method for measurement of glycogen. *Anal. Biochem.* **19:** 315–326.
35. Birk, J. B., and J. F. Wojtaszewski. 2006. Predominant alpha2/beta2/gamma3 AMPK activation during exercise in human skeletal muscle. *J. Physiol.* **577:** 1021–1032.
36. Abbott, M. J., A. M. Edelman, and L. P. Turcotte. 2009. CaMKK is an upstream signal of AMP-activated protein kinase in regulation of substrate metabolism in contracting skeletal muscle. *Am. J. Physiol. Regul. Integr. Comp. Physiol.* **297:** R1724–R1732.
37. Habets, D. D., W. A. Coumans, H. M. El, E. Zarrinpashneh, L. Bertrand, B. Viollet, B. Kiens, T. E. Jensen, E. A. Richter, A. Bonen, et al. 2009. Crucial role for LKB1 to AMPKalpha2 axis in the regulation of CD36-mediated long-chain fatty acid uptake into cardiomyocytes. *Biochim. Biophys. Acta.* **1791:** 212–219.
38. Nickerson, J. G., H. Alkhateeb, C. R. Benton, J. Lally, J. Nickerson, X. X. Han, M. H. Wilson, S. S. Jain, L. A. Snook, J. F. Glatz, et al. 2009. Greater transport efficiencies of the membrane fatty acid transporters FAT/CD36 and FATP4 compared with FABPpm and FATP1 and differential effects on fatty acid esterification and oxidation in rat skeletal muscle. *J. Biol. Chem.* **284:** 16522–16530.
39. Maarbjerg, S. J., S. B. Jorgensen, A. J. Rose, J. Jeppesen, T. E. Jensen, J. T. Treebak, J. B. Birk, P. Schjerling, J. F. Wojtaszewski, and E. A. Richter. 2009. Genetic impairment of AMPKalpha2 signaling does not reduce muscle glucose uptake during treadmill exercise in mice. *Am. J. Physiol. Endocrinol. Metab.* **297:** E924–E934.
40. Shearer, J., P. T. Fueger, B. Vorndick, D. P. Bracy, J. N. Rottman, J. A. Clanton, and D. H. Wasserman. 2004. AMP kinase-induced skeletal muscle glucose but not long-chain fatty acid uptake is dependent on nitric oxide. *Diabetes.* **53:** 1429–1435.
41. Kiens, B., T. H. Roemen, and G. J. van der Vusse. 1999. Muscular long-chain fatty acid content during graded exercise in humans. *Am. J. Physiol.* **276:** E352–E357.
42. Raney, M. A., and L. P. Turcotte. 2006. Regulation of contraction-induced FA uptake and oxidation by AMPK and ERK1/2 is intensity dependent in rodent muscle. *Am. J. Physiol. Endocrinol. Metab.* **291:** E1220–E1227.
43. Raney, M. A., A. J. Yee, M. K. Todd, and L. P. Turcotte. 2005. AMPK activation is not critical in the regulation of muscle FA uptake and oxidation during low-intensity muscle contraction. *Am. J. Physiol. Endocrinol. Metab.* **288:** E592–E598.
44. Rose, A. J., T. J. Alsted, J. B. Kobbero, and E. A. Richter. 2007. Regulation and function of Ca2+-calmodulin-dependent protein kinase II of fast-twitch rat skeletal muscle. *J. Physiol.* **580:** 993–1005.
45. Raney, M. A., and L. P. Turcotte. 2008. Evidence for the involvement of CaMKII and AMPK in Ca2+-dependent signaling pathways regulating FA uptake and oxidation in contracting rodent muscle. *J. Appl. Physiol.* **104:** 1366–1373.
46. Jensen, T. E., A. J. Rose, Y. Hellsten, J. F. Wojtaszewski, and E. A. Richter. 2007. Caffeine-induced Ca(2+) release increases AMPK-dependent glucose uptake in rodent soleus muscle. *Am. J. Physiol. Endocrinol. Metab.* **293:** E286–E292.

Downloaded from www.jlr.org by guest, on June 20, 2012